Comparative Biochemistry and Physiology, Part A 296 (2024) 111695

Contents lists available at ScienceDirect

Comparative Biochemistry and Physiology, Part A

journal homepage: www.elsevier.com/locate/cbpa

Physiological responses of *Holothuria grisea* during a wound healing event: An integrated approach combining tissue, cellular and humoral evidence

Patrícia Lacouth [a], Alessandra Majer [b], Vincenzo Arizza [c], Mirella Vazzana [c], Manuela Mauro [c], Márcio Reis Custódio [a], Vinicius Queiroz [a,*]

[a] Departamento de Fisiologia, Instituto de Biociências, Universidade de São Paulo, Rua do Matão, Trav. 14, n. 101, São Paulo (SP) CEP 05508-900, Brazil
[b] Departamento de Oceanografia Biológica, Instituto Oceanográfico, Universidade de São Paulo, CEP 05508-900 São Paulo (SP), Brazil
[c] Dipartimento di Scienze e Tecnologie Biologiche, Chimiche e Farmaceutiche (STEBICEF), Università di Palermo, Palermo, Italy

ARTICLE INFO

Edited by: Michael Hedrick

Keywords:
Coelomocytes
Cell cooperation
Histology
Coelomic fluid
Tissue repair
Cytology
Cell migration

ABSTRACT

Due to their tissue structure similar to mammalian skin and their close evolutionary relationship with chordates, holothurians (Echinodermata: Holothuroidea) are particularly interesting for studies on wound healing. However, previous studies dealing with holothuroid wound healing have had limited approaches, being restricted to tissue repair or perivisceral immune response. In this study, we combined tissue, cellular and humoral parameters to study the wound healing process of *Holothuria grisea*. The immune responses of the perivisceral coelom were assessed by analyzing the number, proportion and viability of coelomocytes and the volume and protein concentration of the coelomic fluid. Additionally, the morphology of the healing tissue and number of coelomocytes in the connective tissue of different body wall layers were examined over 30 days. Our results showed that perivisceral reactions started 3 h after injury and decreased to baseline levels within 24 h. In contrast, tissue responses were delayed, beginning after 12 h and returning to baseline levels only after day 10. The number of coelomocytes in the connective tissue suggests a potential cooperation between these cells during wound healing: phagocytes and acidophilic spherulocytes act together in tissue clearance/homeostasis, whereas fibroblast-like and morula cells cooperate in tissue remodeling. Finally, our results indicate that the major phases observed in mammalian wound healing are also observed in *H. grisea*, despite occurring at a different timing, which might provide insights for future studies. Based on these data, we propose a model that explains the entire healing process in *H. grisea*.

1. Introduction

The term regeneration has been used broadly to refer to various processes ranging from the repair of a single cell, tissue or organ (Reule and Gupta, 2011; Mahar and Cavalli, 2018) to the growth of an entire organism (Saló and Baguñà, 2002). Traditionally, regeneration is divided into epimorphosis, referring to the replacement of body parts by proliferation of progenitor cells with or without the formation of a blastema (García-Arrarás et al., 2006), and morphallaxis, in which the new tissue is formed from pre-existing cells in the place of injury with no proliferation of progenitor cells (Agata et al., 2007). However, it is clear that regeneration is much more complex and includes processes other than those described by epimorphosis and morphallaxis (Agata et al., 2007; Cigliola et al., 2020). Wound repair is another regenerative process that has sometimes been placed at the same level as regeneration. However, while the wound repair process may be subdivided into hemostasis, humoral and/or cellular inflammation, angiogenesis and generation of mature connective tissue stroma (Dvorak, 2015), regeneration includes additional steps not seen in wound healing (Wong and Whited, 2020).

From an evolutionary perspective, regeneration occurs from sponges to mammals, regardless of phylogenetic position (Ereskovsky et al., 2021; Daponte et al., 2021). Although the cellular and molecular mechanisms of regeneration are well-known in vertebrates (e.g., Daponte et al., 2021), the same is not true for invertebrates, even though some groups have the greatest regenerative potential (Reddien, 2018). Compared to vertebrates, the anatomy and physiological responses of invertebrates are less complex. This aspect can be exemplified by the

* Corresponding author at: Departamento de Fisiologia, Instituto de Biociências, Universidade de São Paulo, Sala 300, Rua do Matão, Travessa 14, n° 101, Cidade Universitária, São Paulo 05508-090, Brazil.
E-mail address: vinicius_ufba@yahoo.com.br (V. Queiroz).

https://doi.org/10.1016/j.cbpa.2024.111695
Received 4 November 2023; Received in revised form 6 July 2024; Accepted 7 July 2024
Available online 9 July 2024

definition of inflammation. In vertebrates, inflammation is a process defined at both macro and micro perspectives (Bergmeier and Wagner, 2007), while it is defined simply as a "cellular migration followed by phagocytosis" in invertebrates (Silva, 2013). This low anatomical and physiological complexity makes them valuable models for regenerative studies. In this context, we highlight the Echinodermata, deuterostome invertebrates found in marine habitats and well-known for their regenerative capabilities (Dupont and Thorndyke, 2007).

Echinoderms have been frequently used as model organisms in several fields, such as cell and developmental biology and immunology (McClay, 2011; Chiaramonte et al., 2019). Regeneration is a widespread and highly developed process in the five main classes of Echinodermata (Thorndyke et al., 2001). In fact, epimorphic and morphallactic regeneration can be easily observed in the arm regeneration of ophiuroids and asteroids, respectively (Dupont and Thorndyke, 2007). Holothurians are also known for their surprising regenerative capabilities, as some species can regenerate their entire digestive tract after evisceration (Ding et al., 2021).

The visceral regeneration in holothurians is a relatively well-studied topic and much of its morphological, cellular, molecular (e.g., Su et al., 2022), physiological (Zang et al., 2012), and even genetic (Zhang et al., 2017) aspects are known. In contrast, other regenerative processes, such as wound healing, remain poorly explored in Holothuroidea. According to Menton and Eisen (1973), "although the regenerative capability of holothurians has been the subject of several studies, the process of cutaneous wound healing in this order has not been subjected to detailed analysis". Even after 50 years, this situation has not significantly changed, with only three studies addressing this issue (viz., Miguel-Ruiz et al., 2007; Vazzana et al., 2015; Mauro et al., 2021). These few studies, although essential for a better understanding of the phenomenon, focus on specific details that follow the event, such as tissue healing/remodeling (Miguel-Ruiz et al., 2007) or physiological/immunological responses (Vazzana et al., 2015; Mauro et al., 2021), and do not provide an integrated view of the responses underlying the wound healing process.

Therefore, in the present study, we performed an integrative morphofunctional approach combining different types of biological parameters (i.e., tissue, cellular and humoral) aiming to obtain a broad understanding of the wound healing process in *Holothuria grisea* Selenka, 1867. Holothurians, like other echinoderms, are deuterostome animals and thus closely related to chordates (Peterson and Eernisse, 2016), with up to 70% of their genes having potential human homologs (Zhang et al., 2017), and well-known for its regenerative capacity (Su et al., 2022). Thus, in addition to providing specific knowledge on the wound healing process in echinoderms, understanding the main mechanisms and responses in this process may offer insights into regenerative medicine, human health, and the evolution of deuterostome regeneration. In addition to characterizing the physiological responses from different perspectives, we also investigate the relationship between the responses in the coelomic and tissue compartments. We hypothesized that specific coelomocyte populations from the perivisceral cavity may be involved in this process, indicating an interrelation between coelomic and tissue compartments during tissue repair. To test this hypothesis, we measured the volume of coelomic fluid, total and differential numbers of coelomocytes, coelomocyte viability, and total number of proteins in the coelomic fluid. Morphological alterations and changes in cell numbers in the affected area were considered tissue responses. Our findings showed that changes in the coelomic fluid were faster, starting from 3 h after injury and finishing after 2 days, while tissue alterations were slower, starting from 12 h after injury and ending after 10 days.

2. Material and methods

2.1. Study animals and experimental design

A total of 132 specimens of *Holothuria grisea* Selenka, 1867 ranging from 13 to 16 cm in length (average 15 cm) were collected in the intertidal zone at the São Sebastião Channel, São Paulo state, Brazil (23°49′462"S 45°24′834"W). They were maintained at room temperature in tanks with running natural seawater and sediment from the collection site. The specimens were acclimated for seven days before the experiments. Experiments were made in duplicate and each experiment used sixty-six specimens, with six for each time point. Out of these six, three specimens were used for physiological analyses (collection of coelomocytes and coelomic fluid) at each time point and three were used for histology.

Using a sterile scalpel (n° 10), an incision of 2 cm piercing down to the coelomic cavity was made longitudinally in the lateral of the body, near the anus, until it reached the perivisceral cavity. After the incision, each animal was kept out of the water for 1–2 min to help close the wound, as they rapidly contract the musculature (and possibly the mutable collagenous tissue) surrounding the injured site, closing it superficially as soon as the damage was done. This mechanism seems to prevent the loss of coelomic fluid and the entry of foreign particles. All animals were then returned to the tanks containing sediment. The animals were evaluated at 1 h, 3 h, 6 h, 12 h and 1, 2, 4, 10, 15 and 30 days after injury. The results were compared to uninjured animals (named 0 h) processed at the beginning of the experiments. Analyses of the coelomic cavity parameters were concentrated at the beginning of the process (1 h to 4 days), while analyses of the tissues started at 12 h after injury up to the thirtieth day (12 h to 30 days). Throughout the experiments, the animals had access to food in the form of sediment from their collection site.

2.2. Coelomic fluid collection, cell counts and trypan blue exclusion assay

The coelomic fluid of the specimens was collected immediately after their removal from the tanks. Each holothurian was removed from the container, allowed to contract and expel water from the respiratory trees, rinsed with water from the container and dried with a paper tissue to avoid contamination of the coelomic fluid (Queiroz et al., 2022a). The coelomic fluid was collected individually through an incision in the anterodorsal region (Vazzana et al., 2015; Mauro et al., 2021) and transferred to a vial containing an ice-cold isosmotic anticoagulant solution in a proportion of 6:1 (ISO-EDTA: 500 mM NaCl, 20 mM Tris–HCl, 30 mM EDTA; pH 7.4 - Mauro et al., 2021) to avoid clotting. The coelomic fluid was then measured in a 25 mL graduated cylinder, discounting the volume of ISO-EDTA added initially and returned to a container with ice until processing for specific analyses. Total cell counts (TCC) were obtained using a Neubauer chamber and cell density was adjusted to 10^6 cells/mL with ISO-EDTA. Differential cell counts (DCC) were performed with the adjusted suspension by counting 100 cells to determine the percentage of each coelomocyte type (DCC = number of a specific cell type / total of cells). The different coelomocyte populations (i.e., phagocytes, progenitor cells, fusiform cells, crystal cells, morula cells, spherulocytes and acidophilic spherulocytes) were identified based on specific literature for *H. grisea* (Queiroz et al., 2022a). Lastly, the adjusted suspension was used to assess cell viability through a trypan blue exclusion assay. For this, 100 μL of the suspension was mixed with an equal volume of trypan blue 0.5%. After five minutes, 100 cells were counted in the Neubauer chamber and the percentage of viable cells was recorded (Freshney, 1987).

2.3. Neutral red uptake assay

For neutral red uptake assay, we followed the protocol of Arizza et al. (2013). Briefly, a suspension of living coelomocytes at 10^6 cells/mL from each sample was prepared in ISO–Ca^{2+} (20 mM Tris, 0.5 M NaCl, 10 mM of $CaCl_2$, pH 7.5). Aliquots of 100 μL (containing 10^5 coelomocytes) were pipetted into three replicates in sterile microplates (96 wells) and allowed to adhere for 30 min. Then, 10 μL of 0.33% neutral red (Sigma-Aldrich) solution in ISO–Ca^{2+} was added to each well and the plates were incubated for 1 h at 10 °C in darkness. The cells were centrifuged at

200 ×*g* for 5 min and washed thrice in ISO–Ca^{2+}. To each well, 100 μL of 1% acetic acid in 50% ethanol was added for the neutral red solubilization. After 15 min, the absorbance of the solution was read at 550 nm in an ELISA plate reader (Molecular Devices Spectramax 250).

2.4. Total protein in coelomic fluid

Total protein analyses were performed using the cell-free coelomic fluid. A sample of 1.5 mL of coelomic fluid was collected from each specimen and centrifuged at 400 ×*g* for 10 min at 4 °C in a clinical centrifuge (Eppendorf 5804-R). The supernatant was removed and stored at −20 °C until analysis. Protein concentration was measured using the Bradford method (Bradford, 1976) at 595 nm.

2.5. Histological analyses

Transverse sections of the body wall (2 cm^2) containing the wounded area of five animals were dissected at each pre-established time point. Body wall sections of five additional uninjured animals (0 h) were used as controls. The samples were fixed for 24 h at room temperature in glutaraldehyde 2.5% in sterile-filtered seawater (0.22 μm) and decalcified with EDTA 5% in Ca/Mg-free artificial seawater (NaCl 460 mM, Na_2SO_4 7 mM, KCl 10 mM, HEPES 10 mM, pH 8.2 - Dunham and Weissmann, 1986). The tissues were then dehydrated through a graded ethanol series (50–100%), followed by xylene, and embedded in Paraplast (Sigma) following usual procedures (Behmer et al., 1976). Histological sections, 7 μm thick, were made using a manual microtome (AO820, American Optical) and stained with Mallory's trichrome (Behmer et al., 1976). Cells in the sections were identified based on specific literature on echinoderms (Cowden, 1968; Menton and Eisen, 1973; Byrne, 1986; Lunetta and Michelucci, 2001; Miguel-Ruiz et al., 2007; Sugni et al., 2014; Eisapour et al., 2021) and, when possible, correlated with the morphology of living coelomocytes in the coelomic fluid (Xing et al., 2008; Queiroz et al., 2022a). Cell counts were performed on digital photographs taken on both sides of the wound canal in three histological sections from each animal analyzed. Three random fields were evaluated in each body wall region (superficial, central and hypodermis). Cell counts on histological sections varied between 500 and 1100 cells per time point, considering all replicates.

2.6. Data presentation and statistical analyses

Results from the parameters analyzed in the perivisceral coelomic fluid, such as volume of coelomic fluid, total and differential cell counts, trypan blue exclusion, neutral red uptake and total protein concentration, are presented as mean ± standard deviation. One-way analysis of variance (ANOVA) was used to analyze the differences between the various time points. Holm-Sidak's multiple comparisons post hoc tests were applied to one-way ANOVA when necessary to identify which time points differed from the injured group. Statistical analyses of the coelomic fluid parameters were performed using GraphPad Prism 7.

The difference in the number of cells in the histological analyses was tested by a factorial ANOVA, considering the cell type (fibroblast-like cells, phagocytes, morula cells or acidophilic spherulocytes), dermal position (superficial, central or hypodermis) and the time points for regeneration (0 h, 12 h and 1, 2, 4 10, 15 and 30 days). This was followed by a post hoc Tukey's test to detect significant differences in pairwise comparisons. Because the data did not meet the criteria for normality or homoscedasticity, a logarithmic transformation was applied (ln(n + 1)). Since the cells were sparsely distributed in the matrix, the results are given as cells per area of a photographed field at 400× magnification (67,600 $μm^2$–300 μm length × 225 μm width) instead of relative participation (%), as this better reflects the fluctuations of each population during the experiments.

3. Results

3.1. Physiological responses in the perivisceral coelomic fluid

The response in the coelomic fluid was evaluated through six parameters: coelomic fluid volume, total and differential coelomocyte counts, trypan blue exclusion and neutral red uptake assays, and total protein concentration in the cell-free coelomic fluid. The volume of coelomic fluid, used to assess how the healing process affected the regulation of perivisceral fluid volume, was 9.66 ± 1.63 mL in uninjured animals (0 h). The mean volume increased at 1 h and 3 h post-injury, but was only significantly different from the uninjured animals at 6 h after injury (17.25 ± 3.06 mL) (Fig. 1). Twelve hours post-injury, the volume returned to values close to those of uninjured animals, but significantly increased one day after injury (15.17 ± 4.15 mL) (Fig. 1). From the second day onwards, the volume reached values similar to those of uninjured animals (Fig. 1).

Total cell counts, used to measure changes in the number of coelomocytes in the coelomic cavity, were higher in uninjured animals (8.57 ± 0.68 × 10^6 cells/mL) and significantly decreased at 1 h and 3 h post-injury. Cell counts reached values close to those of uninjured animals at 6 h after injury, but then significantly decreased 12 h and one day post-injury (Fig. 2A). Two days after injury, cell counts increased to 5.40 ± 0.88 × 10^6 cells/mL, but this was still significantly different from the values of uninjured animals. On the fourth day, the total cell count was close to that of uninjured animals (Fig. 2A).

Differential cell counts were employed to investigate alterations in different coelomocyte populations, which may vary considerably. The only cell types with some difference from the uninjured organisms were phagocytes, progenitor cells and fusiform cells. One hour after injury, the percentages of phagocytes and progenitor cells, which are the most common cells in the coelomic fluid of *H. grisea*, were similar to those of uninjured animals (Fig. 2B and Supplementary Table 1). However, the percentages of phagocytes significantly decreased at 3 h and 12 h (Fig. 2B and Supplementary Table 1), while progenitor cells increased consistently, reaching a peak at 6 h ($p < 0.05$) and then decreasing again to values close to those of uninjured animals (Fig. 2B and Supplementary Table 1). Fusiform cells remained close to 2% and usually did not increase >4%, except on the fourth day, in which they increased above this value and significantly differed from the numbers observed in uninjured animals (Fig. 2C and Supplementary Table 1). Crystal cells, morula cells, acidophilic spherulocytes and spherulocytes varied in percentage during the early regeneration, but did not differ significantly from the numbers observed in uninjured animals (Fig. 2C and D and Supplementary Table 1).

The cell integrity and viability, as measured by trypan blue exclusion and neutral red uptake assays, showed contrasting results. In the trypan blue exclusion assay, the coelomocyte viability of uninjured animals was 84.05 ± 4.17%, increasing slightly 1 h post-injury (Fig. 3). This value significantly decreased at 3 h post-injury and returned to values close to those of uninjured animals at 6 h and 12 h post-injury (Fig. 3). Cell viability significantly decreased again one day after injury (68.19 ± 8.54%) and returned to values similar to those observed for uninjured animals on the second and fourth days (Fig. 3).

For the neutral red uptake, the pattern was completely different from the previous assay (Fig. 4). Uninjured animals showed the highest capability of accumulating neutral red, with optical densities of 0.140 ± 0.025 at 550 nm. This ability significantly decreased by 35.7 and 50% compared to uninjured animals during the first three hours (Fig. 4). At 6 h and 12 h, the values significantly decreased by 28.5 and 57.1%, reaching the lowest value one day post-injury (0.060 ± 0.006), when compared to uninjured animals. Two days after injury, the values increased slightly compared to one day post-injury, but were still 28.5% lower than those observed for uninjured animals (Fig. 4). It was only on the fourth day that the values approached those observed for uninjured animals, but even then, they were significantly lower (Fig. 4).

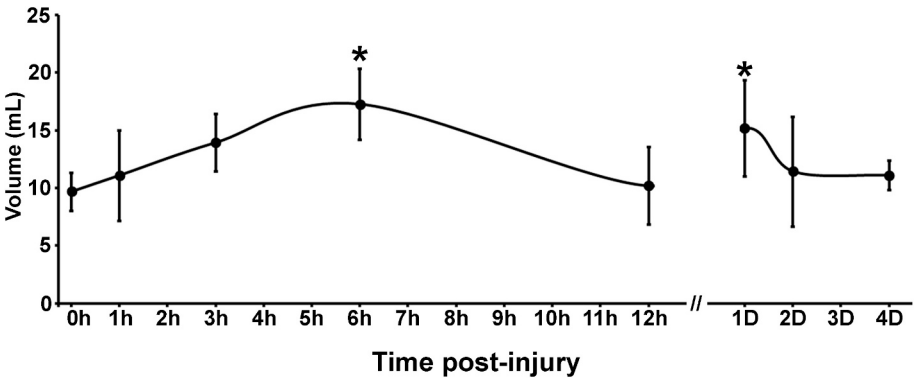

Fig. 1. Volume of perivisceral coelomic fluid of *Holothuria grisea* at different times post-injury. Black bars indicate mean ± standard deviation. Asterisks indicate significant differences ($p < 0.05$) between time points and uninjured animals (0 h) in One-Way ANOVA.

The total protein concentration in the cell-free coelomic fluid is traditionally used to address humoral proteins. Uninjured animals showed 0.25 ± 0.11 mg/mL of total protein, which significantly increased 1 h post-injury (Fig. 5). At 6 h, 12 h, and one day post-injury, total protein was also significantly higher when compared to uninjured animals. Protein concentration peaked after two days, with values of 0.59 ± 0.07 mg/mL ($p > 0.05$), and started to decrease on the fourth day (Fig. 5).

3.2. Physiological responses in the injured area

Tissue morphology and different cell type numbers were evaluated in order to understand the physiological dynamics of the healing process. The uninjured body wall of *H. grisea* was composed of: a thin cuticle; an epidermis, which is characterized by an epithelium similar to the mammalian pseudo-stratified one; and a dermis, divided into superficial, central and hypodermis, which was distinguished by the thickness and general orientation of the collagen fibers (Fig. 6A and 7A). The superficial dermis consisted of loose connective tissue, large amounts of ground-like substance – as defined for vertebrates and sea cucumbers (Vázquez-Vélez et al., 2016; McMillan and Harris, 2018) – and thin collagen and elastic fibers. The central dermis showed dense irregular connective tissue, rich in thick and irregularly arranged collagen fibers. Lastly, the hypodermis was similar to the superficial dermis and was limited by the coelomic epithelium and circular muscle fibers. Only four cell types were observed in these layers, three of them named according to their morphological and cytochemical similarity with coelomic cells (Queiroz et al., 2022a). Fibroblast-like cells were characterized by an elliptical and acidophilic nucleus (4 μm in diameter) and filopodia extending from the cytoplasm (Fig. 6B). Phagocytes were spherical cells with a hyaline and vacuolated cytoplasm (Fig. 6C). Morula cells and acidophilic spherulocytes (Fig. 6D) were named according to their morphology and stain affinity in Mallory's Trichrome (Queiroz et al., 2022a).

A few minutes after the injury, both sides of the superficial layer underwent a localized contraction and the wound borders were macroscopically closed. However, a slight pressure over the area could easily reopen the cut. Histological analyses from 1 h, 3 h and 6 h post-injury (data not shown) displayed the same pattern observed for 12 h and were therefore disregarded. The first histological analysis post-injury (12 h – Fig. 7B) revealed that only the epithelial tissue and the superficial dermis were in contact, closing the external aperture, but the internal wound canal was still open (Fig. 7B). Morula cells, phagocytes and fibroblast-like cells were observed inside the wound canal (Fig. 7B *inset* and Supplementary Fig. 1). At this stage, the number of fibroblast-like cells in the superficial dermis was reduced to one-third of that observed in the uninjured animals (from 19.5 ± 6.4 to 6.5 ± 2.9, $p < 0.0001$. Supplementary Table 2) and the number of phagocytes significantly increased in the hypodermis ($p = 0.006$). Despite a slight decrease in fibroblast-like cells ($p = 0.003$), no significant alterations occurred in the central dermis. However, the number of morula cells doubled in the hypodermis (from 8.8 ± 5.1 to 18.6 ± 6.3, $p < 0.01$) (Fig. 8 and Supplementary Table 3).

Twenty-four hours after the injury, the sides of the wound canal were in contact, especially in the superficial region (Fig. 7C). Some cellular necrosis and degeneration of the extracellular matrix were observed in the superficial dermis. In this region, fibroblast-like cells began to recover to their original levels and could be observed interspersed with epithelial cells. During this time, phagocytes were found in larger numbers in the central dermis ($p < 0.0001$) (Supplementary Table 3) and started to decline in the hypodermis (Fig. 8 and Supplementary Table 3). Also in the hypodermis, morula cells were reduced closer to the numbers found in normal tissues (Fig. 8 and Supplementary Table 3), but could still be observed inside the wound canal alongside a few fibroblast-like cells (Fig. 7C *inset* and Supplementary Fig. 1).

Two days after the injury (Fig. 7D), clear disorganization was observed from the epithelium down to the central dermis, with phagocytes, acidophilic spherulocytes and debris present in the area (Fig. 7D *inset*). At this stage, the number of fibroblast-like cells in the superficial and central dermis reached the original levels found in uninjured tissues ($p = 0.99$ for both comparisons – Fig. 8 and Supplementary Table 3) and thin collagen fibers started to close the canal from the central dermis region (Fig. 7D *inset* and Supplementary Fig. 1). Morula cells were still observed in the wound canal and hypodermis, but in much lower numbers compared to their 12 h peak ($p < 0.001$) (Fig. 8 and Supplementary Table 3).

There were no signs of external injury on the fourth day, but a disorganized area was still visible in the epidermis and superficial dermis (Fig. 7E). The wound canal in the central dermis and hypodermis was sealed with many new collagen fibers (Fig. 7E). These were thinner and organized perpendicularly to those in the surrounding matrix, making the wound canal easily distinguished internally. The occurrence of fibroblast-like cells increased in the central dermis and hypodermis ($p < 0.001$ for both comparisons – Fig. 8 and Supplementary Table 3). On the other hand, the phagocyte number decreased in the hypodermis, but showed a tendency to increase in the superficial dermis ($p < 0.0001$ for both comparisons – Fig. 8 and Supplementary Table 3). Notably, a marked increase of acidophilic spherulocytes was observed in the superficial and central dermis, while morula cells were reduced to the lowest levels observed during the experiment (Fig. 8 and Supplementary Table 3).

Ten days after the injury, a new layer of epidermal cells was fully formed, but the fibers in the superficial dermis were still disorganized and mingled with those in the central dermis (Fig. 7F). At this phase, the thickness of the new fibers that filled the wound canal resembled those in the normal tissue (Fig. 7F). Fibroblast-like cells were restricted to the

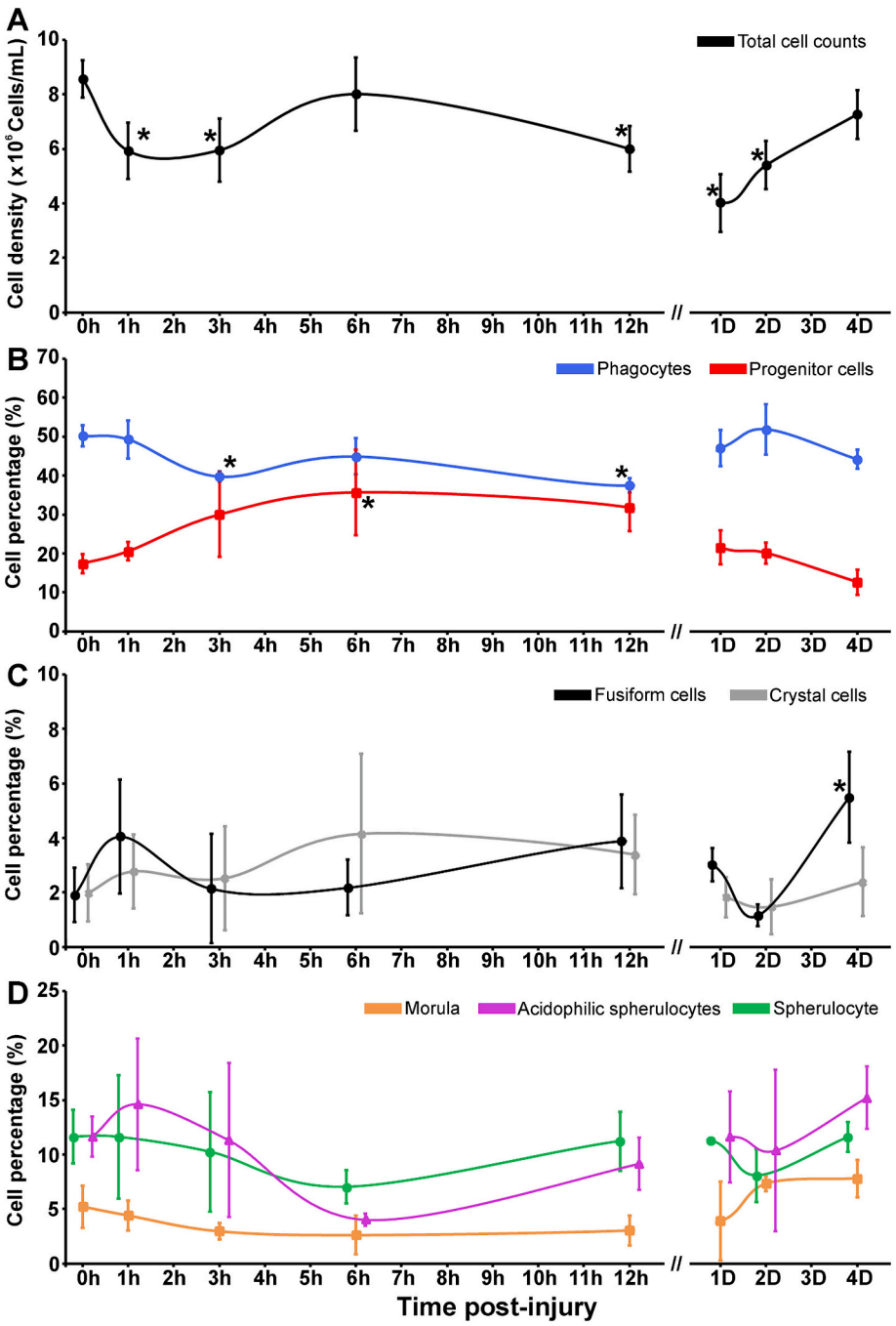

Fig. 2. Coelomocyte counts of *Holothuria grisea* at different times post-injury. A – Total cell counts; B–D – Differential cell counts highlighting the percentages of phagocytes and progenitor cells (B); Fusiform cells and Crystal cells (C); and the different spherule cell populations (D). Bars indicate mean ± standard deviation. Asterisks indicate significant differences ($p < 0.05$) between time points and uninjured animals (0 h) in One-Way ANOVA.

superficial dermis and numerically similar to normal tissues ($p = 0.99$), while phagocytes were almost absent from the three layers (Fig. 8 and Supplementary Table 3). Acidophilic spherulocytes in the superficial and central dermis were markedly reduced compared to the previous stage (four days – $p < 0.001$ for both comparisons – Fig. 8 and Supplementary Table 3) and only a few intact cells could be detected. However, debris and many extracellularly located spherules with similar cytochemical characteristics were observed in the wound canal region. The number of morula cells doubled over the previous period and was closer to normal levels ($p = 0.99$ for all three comparisons – Fig. 8 and Supplementary Table 3).

On the fifteenth day (Fig. 7G), the differentiation between the superficial and central dermis was visible again and the wound canal was fully occupied by collagen fibers, which still maintained a perpendicular orientation compared to the surrounding matrix (Fig. 7G). In the superficial dermis, phagocytes returned to the levels observed in uninjured animals. After this stage, there were no significant modifications of the cell numbers or tissue organization (Fig. 8 and Supplementary Table 3) and, on the thirtieth day, the region was completely restructured (Fig. 7H). The body layers were clearly differentiated, although it was still possible to notice a scar where the lesion was made (Fig. 7H). The numbers of fibroblast-like cells and phagocytes were similar to those of uninjured animals. Nevertheless, the number of acidophilic spherulocytes in the hypodermis remained slightly higher than in normal

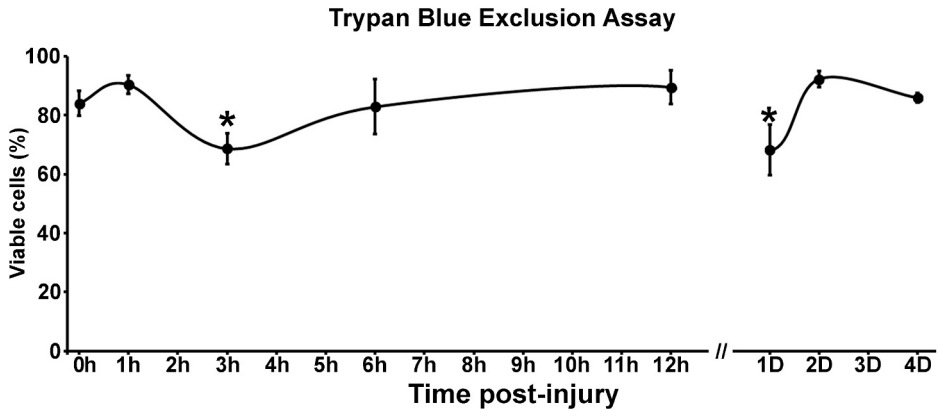

Fig. 3. Coelomocyte viability of *Holothuria grisea* through trypan blue exclusion assay at different times post-injury. Black bars indicate mean ± standard deviation. Asterisks indicate significant differences ($p < 0.05$) between time points and uninjured animals (0 h) in One-Way ANOVA. (For interpretation of the references to colour in this figure legend, the reader is referred to the web version of this article.)

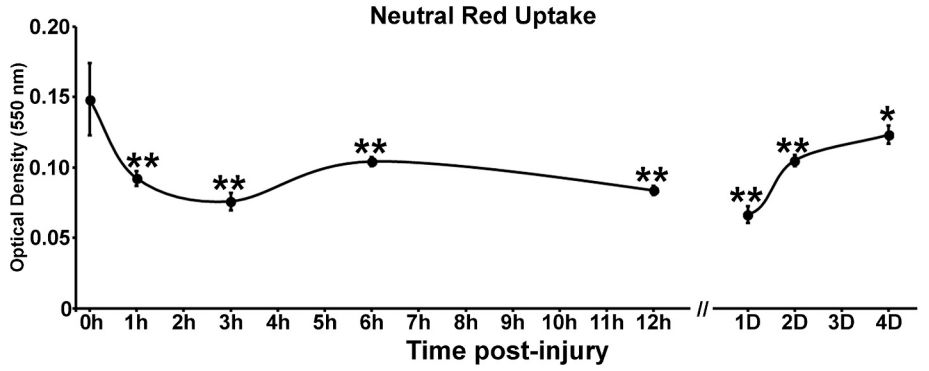

Fig. 4. Neutral red uptake of *Holothuria grisea's* coelomocytes at different times post-injury. Black bars indicate mean ± standard deviation. Asterisks indicate significant differences between time points and uninjured animals (0 h) in One-Way ANOVA. One asterisk (*) indicates $p < 0.05$, and two asterisks (**) indicate $p < 0.01$. (For interpretation of the references to colour in this figure legend, the reader is referred to the web version of this article.)

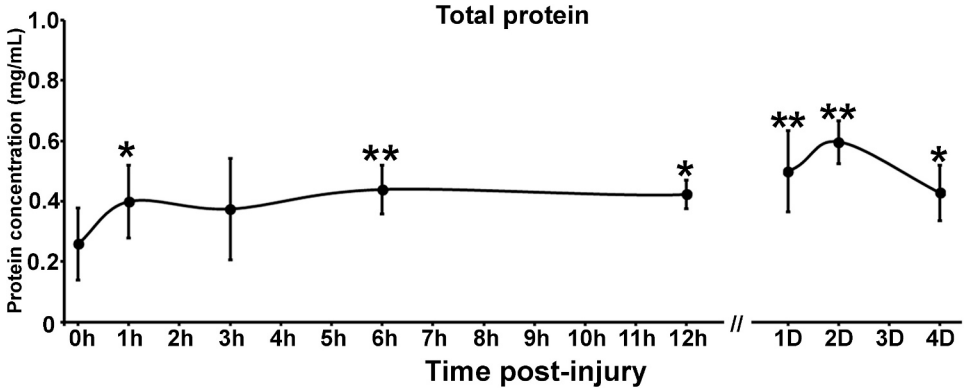

Fig. 5. Protein concentration of cell-free coelomic fluid of *Holothuria grisea* at different times post-injury. Black bars indicate mean ± standard deviation. Asterisks indicate significant differences between time points and uninjured animals (0 h) in One-Way ANOVA. One asterisk (*) indicates $p < 0.05$, and two asterisks (**) indicate $p < 0.01$.

tissues ($p < 0.0001$ – Fig. 8 and Supplementary Table 3).

4. Discussion

Overall, our results show that the physiological responses of *H. grisea* during a wound-healing event are quite complex, being both place- and time-dependent. Some effects, such as total cell counts, may be seen 1 h post-injury. Cellular and humoral parameters, measured at the beginning of the healing process, exhibit the same general pattern: most responses become clearer at 3 h and one day post-injury, reverting to the levels of uninjured animals within two days. In contrast, tissue responses are delayed compared to coelomic ones, being observed 12 h post-injury, extending to the fourth day and returning to basal levels only on the tenth day post-injury. We also observe cooperation among tissue coelomocytes during the healing process, with phagocytes and acidophilic spherulocytes being involved in homeostasis while fibroblast-like cells and morula cells are involved in remodeling and tissue growth. Details of the responses of each compartment and the integration of

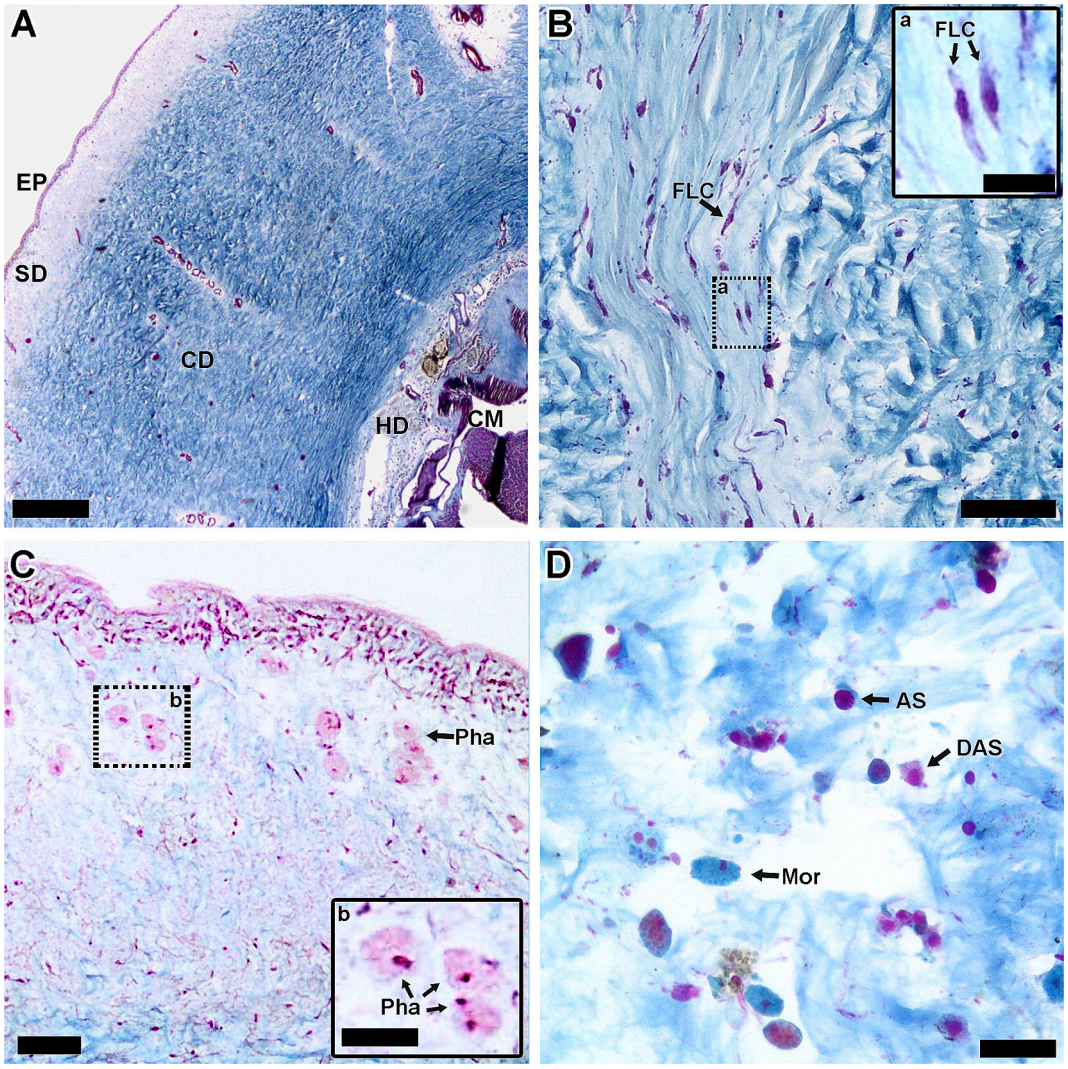

Fig. 6. Tissue organization and cells present in the body wall of *Holothuria grisea*, stained with Mallory's trichrome. A – Histological section of *Holothuria grisea* body wall highlighting the epidermis (EP), superficial dermis (SD), central dermis (CD), hypodermis (HD), and circular muscles (CM). B – Fibroblast-like cells in the central dermis; B *inset* – Fibroblast-like cells in detail. C – Phagocytes in the superficial dermis; C *inset* – Phagocytes in detail. D – Spherule cells in the central dermis, highlighting the morula cells and the two morphologies of acidophilic spherulocytes: undegranulated and degranulated. Legend: AS = undegranulated acidophilic spherulocyte; DAS = degranulated acidophilic spherulocyte; FLC = fibroblast-like cell; Mor = Morula cell; Pha = Phagocyte. A = 500 μm; B and C = 50 μm; C *inset* and D = 25 μm; B *inset* = 12,5 μm.

tissue coelomocytes during the healing process will be further addressed in specific sections below.

4.1. Physiological responses in the perivisceral coelom

The coelomic fluid volume of *H. grisea* consistently increases during the wound healing event, reaching its highest values at 6 h and one day post-injury and returning to pre-injury levels from the second day on. As demonstrated by previous studies addressing osmoregulation in the asteroids *Luidia clathrata* and *Odontaster validus* (Pearse, 1967; Ellington and Lawrence, 1974), echinoderms are known for their ability to regulate perivisceral coelomic fluid volume. Coelomic fluid volume regulation has been identified as the first step during intestinal regeneration in Holothuroidea (Dolmatov, 2021) and a recent study using *Holothuria tubulosa* showed that the volume decreases during wound healing (Mauro et al., 2021). In addition to being the area in which most physiological responses occur (e.g., phagocytosis – Ramírez-Gómez et al., 2010), the perivisceral coelomic fluid also functions as a hydrostatic skeleton, providing support during locomotion. A plausible explanation for the difference in the general pattern of coelomic fluid volume during the wound healing of *H. grisea* and *H. tubulosa* may come from their specific behaviors during the process. Vazzana et al. (2015) observed that *H. tubulosa* contracts and shortens its body during wound healing. In contrast, *H. grisea* spends most of its time motionless, with an elongated body in a relaxed state. Thus, the repeated contractions of *H. tubulosa* may expel fluid from its body, decreasing coelomic fluid volume, while the relaxed state of *H. grisea* contributes to filling its perivisceral cavity. However, this information is based on few observations, as we did not consistently observe the behavior of *H. grisea* during wound healing, and further analyses should be performed to confirm our hypothesis.

Total and differential cell counts have been previously used to assess the physiological state of invertebrates (Kale and Krishnamoorthy, 1979; Silva et al., 2002; Queiroz, 2020). In *H. grisea*, total cell count (TCC) decreases during the wound healing process, reaching its lowest values one day post-injury and returning to pre-injury levels on the fourth day. Total cell counts increase in organisms submitted to different physiological stresses, such as exposure to lipopolysaccharides (Chiaramonte et al., 2019), gram-negative bacteria (Yui and Bayne, 1983), osmotic stress, handling (Shannon and Mustafa, 2015) and even during

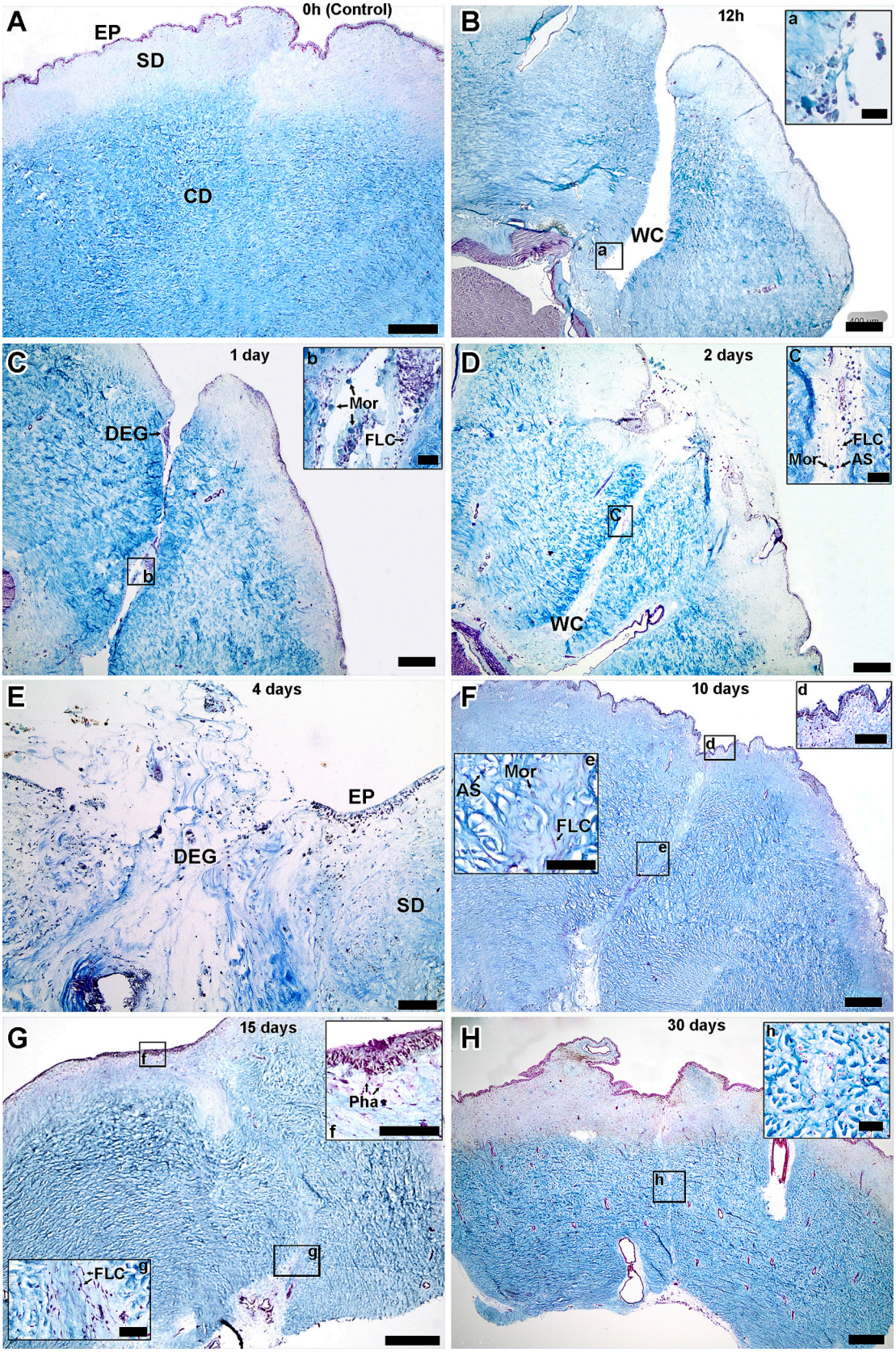

(caption on next page)

Fig. 7. Histological sections of the injured body wall of *Holothuria grisea* at different times post-injury. A – Body wall of uninjured animals (0 h); B – Injured area at 12 h, highlighting the opened wound canal and the cells close to the wound border (B *inset*); C – Injured area at 24 h, highlighting the partially closed wound canal and the cells in the area (C *inset*); D – Injured area at 2 days, highlighting the partially closed wound canal, the beginning of the cicatrization (thin fibers in the wound canal), and the high number of cells in the area (D *inset*); E – Injured area at 4 days, highlighting a closed wound canal, and the initial cicatrization of the area (disorganized fibers in the wound canal); F – Injured area at 10 days, highlighting a completely closed wound canal, a formed epidermis (F *inset d*), and the different organization of the fibers in the wound canal (F *inset e*)initial cicatrization of the area (disorganized fibers in the wound canal); G – Injured area at 15 days, highlighting the fibers in the connective tissue that still maintain a perpendicular orientation in relation to the surrounding matriz (G *inset g*). Note the completely formed epidermis and the phagocytes in the place of the wound canal (G, *inset f*). The Injured area at 30 days, highlighting a healing process almost finished and the organization of the fibers in the connective, which is quite similar to the uninjured area (H *inset*). Legend: EP = epidermis; SD = superficial dermis; CD = central dermis; WC = wound canal; DEG = degenerated area; AS = acidophilic spherulocyte; FLC = fibroblast-like cell; Mor = morula cell; Pha = phagocyte. Scales: A-H, *Inset d*, and *Inset f* = 400 μm; *Inset a* = 25 μm; *Inset b*, *Inset c*, *Inset g*, and *Inset h* = 50 μm; *Inset e* = 100 μm.

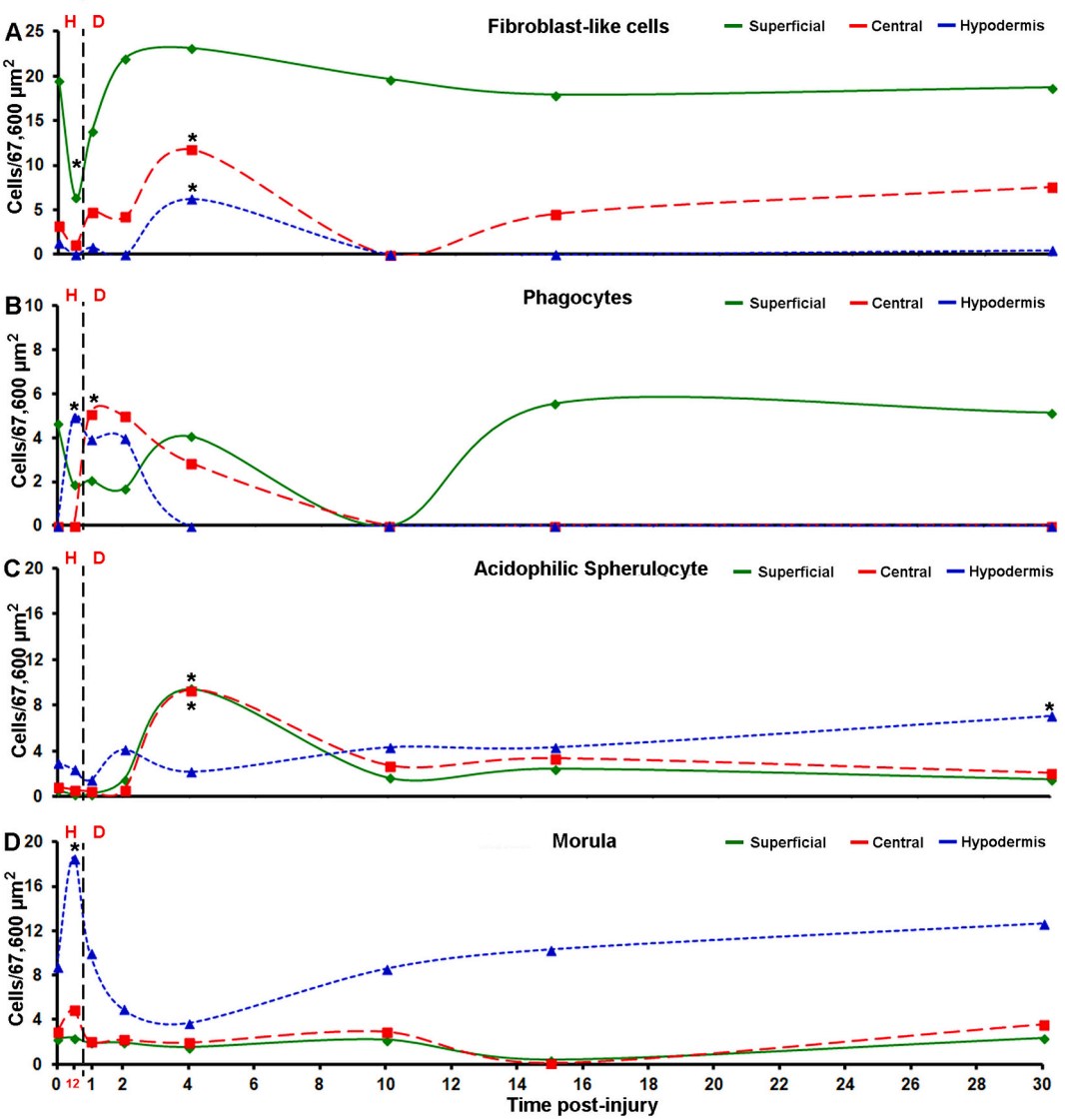

Fig. 8. Mean number of fibroblast-like cells (A), phagocytes (B), acidophilic spherulocytes (C), and morula cells (D) observed in the injured dermis (superficial, central, and hypodermis) of *Holothuria grisea* at different times post-injury. Zero hours (0 h) values consist of cell counts in uninjured animals (0 h). Error bars were omitted for clarity, and points with statistically significant changes concerning the uninjured animals ($p < 0.05$) are indicated by asterisks. Mean and standard deviations for these counts may be seen in Supplementary Table 3. The black dashed line (and red letters) separates the time in hours (H) from the time in days (D). (For interpretation of the references to colour in this figure legend, the reader is referred to the web version of this article.)

interactions with other invertebrates or predators (Queiroz, 2020; Hamel et al., 2021). Conversely, a reduction in total cell counts is also detected during regenerative events in *H. tubulosa* and *Apostichopus japonicus*, corroborating the pattern observed in *H. grisea* herein (Vazzana et al., 2015; Li et al., 2018). Regarding differential cell counts (DCC), phagocytes, progenitor cells and fusiform cells are the only coelomocyte populations in which significant differences are observed during the wound healing process in *H. grisea*. Phagocytes are usually the most responsive perivisceral coelomocytes in Echinodermata, increasing in numbers during different types of challenges, as observed in sea urchins (Shannon and Mustafa, 2015; Chiaramonte et al., 2019) and sea cucumbers (Ramírez-Gómez et al., 2010; Shannon and Mustafa,

2015; Hamel et al., 2021). However, the proportion of phagocytes decreases during the wound healing process in *H. grisea*, reaching its lowest values at 3 h and 12 h post-injury. This is similar to what has been observed during regeneration in *H. tubulosa* and *Apostichopus japonicus*, in which the lowest values of phagocytes (filopodial ones in *H. tubulosa*) were measured around 2 h and 6 h post-injury (Vazzana et al., 2015; Li et al., 2018). In turn, progenitor cells are typical holothurian coelomocytes that are speculated to be circulating stem cells (Queiroz and Custódio, 2024) and few previous studies have assessed them during DCC (Ramírez-Gómez et al., 2010; Prompoon et al., 2015; Vazzana et al., 2015; Li et al., 2018). In *H. grisea*, an increase in progenitor cells was observed 12 h post-injury. A similar pattern was observed only after 24 h in *H. tubulosa*, although significant differences were not detected in that species (Vazzana et al., 2015). All these data show that the patterns observed during regeneration might differ from those observed during other types of stress.

The differences observed in the general pattern of TCC and DCC during the wound healing process compared to other types of physiological stress may be explained by considering the putative fate of the cells. In other types of stress, the animal needs to cope with the imbalance in the coelom by increasing phagocytosis or cytotoxic activity (Yui and Bayne, 1983; Vazzana et al., 2018). During a wound healing event, in addition to coping with such physiological imbalances, the coelomocytes may be providing support in tissue responses, which could explain their decrease in the perivisceral coelom. This explanation matches what was observed in the case of a bryozoan *Schizoporella errata* encrusting the test of the sea urchin *Echinometra lucunter* (Queiroz, 2020), in which red spherulocytes were observed to accumulate at the wound site in addition to their increase in the coelomic fluid.

Trypan blue and neutral red assays are commonly used to study the physiological state of cells and both methods have been applied to vertebrates and invertebrates, and are based on simple principles (Arizza et al., 2013; Melo et al., 2019). Viable cells (1) exclude trypan blue dye from their cytoplasm if their membranes are intact (Strober, 2015) or (2) actively uptake and maintain neutral red dye inside lysosomes if this organelle is functional (Ates et al., 2017). Although the specific tendencies differ in the present study, both assays show a similar pattern: cell viability reaches the lowest values at 3 h and one day post-injury (Fig. 4 and Fig. 5). Coelomocyte viability measured through trypan blue is typically above 90%, as observed in echinoids (Figueiredo et al., 2016; Stabili et al., 2018; Queiroz et al., 2022b) and asteroids (Stabili et al., 2018). However, values of 88.3% and 80% are also observed in supposedly healthy cells (Stabili et al., 2018; Murano et al., 2021), similar to those observed in uninjured specimens of *H. grisea*. Other studies also show that coelomocyte viability measured through neutral red uptake decreases after a physiological stress, such as long-term maintenance of cell cultures, spawning stress and exposure to chemical substances, as observed in the sea urchin *P. lividus* (Arizza et al., 2013; Pinsino and Alijagic, 2019; Murano et al., 2021).

Although the use of both viability assays seems redundant, the integration of these methods provides a better understanding of coelomocyte physiology and, consequently, of the wound healing process. For example, except for 3 h and one day post-injury, all other time points show results similar to those of uninjured animals in the trypan blue assay. However, the results of all time points in the neutral red assay are lower than those of uninjured animals. Since the trypan blue assay is based on membrane integrity, the membrane may be intact during the analyses, but the cell is in the process of programmed cell death (apoptosis), which will certainly change the baseline cell physiology. A recent study with cultured cells of the sea urchin *P. lividus* properly illustrated this situation, with cell viability measured by trypan blue and neutral red showing divergences (Pinsino and Alijagic, 2019). Moreover, these are fast and inexpensive physiological assays that are accessible to most researchers. Thus, as the physiological condition may not be fully understood by using only one of these parameters, we suggest using a combination of both methods to achieve a more complete view of coelomocyte viability whenever possible.

Total protein concentration in the coelomic fluid has also been used to investigate various types of physiological stresses in echinoderms, such as diseases, noise pollution, reproductive cycles and bacterial challenges (Jellett et al., 1988; Ura et al., 2017; Vazzana et al., 2020; Wahltinez et al., 2020). Here, we observe that the total protein concentration increases throughout the wound healing process, reaching its highest values on the second day post-injury and starting to return to pre-injury levels only on the fourth day. Similar changes in total protein concentration are observed in protozoa-infected *Strongylocentrotus droebachiensis* and in bacteria-infected *Evechinus chloroticus* (Jellett et al., 1988; Johnstone, 2015), and throughout the evolution of wasting syndrome disease in *Pisaster ochraceus* (Wahltinez et al., 2020). This increase may be mediated by different but complementary processes. For example, acidophilic spherulocytes from *H. tubulosa* and colorless spherulocytes from *P. lividus* are known for their cytotoxic activity, releasing lysins/hemolysins that act against foreign particles (Arizza et al., 2007; Vazzana et al., 2018). Esterase, peroxidase, alkaline phosphatase (Mauro et al., 2021), complement-like proteins, *Sp* Transformer proteins (Clow et al., 2004; Chou et al., 2018) and agglutinins (Canicattì and Parrinello, 1985; Canicattì, 1988) are also known to increase after stressful situations. The specific events that trigger this response in *H. grisea* need to be further studied, but it is necessary to keep in mind that different physiological processes may be occurring in this scenario: perivisceral coelom clearance/defense and tissue healing and growth. In any case, the evaluation of total protein concentration effectively demonstrates physiological alterations.

4.2. Physiological responses in the injured tissue

Several studies have characterized the body wall of sea cucumbers (Cowden, 1968; Menton and Eisen, 1970, 1973; Byrne, 1986; Lunetta and Michelucci, 2001; Miguel-Ruiz et al., 2007; Guerrero and Forero, 2018), aiming to understand: (1) how the dermis is organized, (2) the primary cell types present in each layer, and (3) how these cells behave during stressful situations. These parameters can be used to understand the physiological dynamics of the tissue during a wound healing event. The body wall of *H. grisea* has a four-layered structure composed of epidermis, superficial dermis, central dermis and hypodermis, which corresponds to the body wall structure observed in the holothurians *Isostichopus* aff. *Badionotus, Eupentact quiquesemita* and *Sclerodactyla briaureus* (Menton and Eisen, 1970, 1973; Byrne, 1986; Guerrero and Forero, 2018). In *H. grisea,* the superficial dermis and hypodermis are characterized mainly by their loose connective tissue bearing large amounts of ground substance, while the central dermis is composed of a dense connective tissue rich in thick and irregularly arranged collagen fibers, corroborating the data from previous studies (Menton and Eisen, 1970, 1973; Byrne, 1986; Guerrero and Forero, 2018).

The cells observed in the dermis of *H. grisea* (or “connective coelomocytes”, as proposed by Cowden, 1968) correspond to those found in the tissue and perivisceral coelom of other echinoderms. The fibroblast-like cells of *H. grisea* are also observed in the sea cucumbers *Isostichopus badionotus* and *Sclerodactyla briaureus* and in the sea urchin *Paracentrotus lividus* (Cowden, 1968; Menton and Eisen, 1973; Sugni et al., 2014). Curiously, fibroblast-like cells are morphologically similar to the perivisceral fusiform cells found in other holothuroids (Xing et al., 2008; Queiroz et al., 2022a). The connective phagocytes of *H. grisea* are morphologically similar to those observed in the tissues of *H. parva* (Eisapour et al., 2021, named “amoebocytes”) and the perivisceral phagocytes of *A. japonicus*, *H. glaberrima, H. grisea*, *H. arenicola* and *H. tubulosa* (Taguchi et al., 2016; Ramírez-Gómez et al., 2010; Queiroz et al., 2022a). Cells morphologically similar to perivisceral spherule cells have been found embedded in the connective tissue of holothurians. However, most studies dealing with connective spherule cells of sea cucumbers (e.g., Menton and Eisen, 1970, 1973; Byrne, 1986; Lunetta and Michelucci, 2001; Miguel-Ruiz et al., 2007; Guerrero and

Forero, 2018) have reported only one cell type, which is morphologically similar to the perivisceral morula cell recently recorded for *H. grisea* (Queiroz et al., 2022a). On the other hand, coelomocytes corresponding to acidophilic spherulocytes are only observed in the body wall of *H. glaberrima* and *H. polii* (Lunetta and Michelucci, 2001; Miguel-Ruiz et al., 2007). The morula cell and acidophilic spherulocytes in the connective tissues of *H. grisea* show the same morphological and cytochemical characteristics of perivisceral coelomocytes in *A. japonicus*, *Cucumaria japonica, H. arenicola, H. tubulosa*, *H. glaberrima* and *H. grisea* itself (Eliseikina and Magarlamov, 2002; Ramírez-Gómez et al., 2010; Queiroz et al., 2022a). Thus, our results show that the cell diversity observed in *H. grisea* tissues matches the cells observed in other holothurians.

For a broad understanding of the connective coelomocyte dynamics and the wound healing process, it is necessary to consider that two different but complementary physiological responses occur simultaneously: while processes responsible for maintaining systemic homeostasis (e.g., phagocytosis and cytotoxic activity) stand out, the animal must also manage tissue healing and remodeling. In the former, the activity of connective phagocytes and acidophilic spherulocytes is significant. In Holothuroidea, these cells are involved in the elimination of particles and cytotoxic activity, respectively (Kun and Yang, 2009; Vazzana et al., 2018). Phagocytes from the superficial dermis decrease significantly in number during the first two days post-injury, returning to pre-injury levels on the fourth day and stabilizing only on the 15th day. Meanwhile, phagocytes from the central dermis and hypodermis show a different pattern, increasing in the first two days post-injury and starting to return to pre-injury levels from the fourth day on. In the case of acidophilic spherulocytes, the pattern was opposite to that of phagocytes. The first change is observed in the hypodermis, where acidophilic spherulocytes continually decrease, reaching their lowest values one day post-injury. Then, their number sharply increased on the 2nd day, returning to pre-injury levels by the 4th day. Meanwhile, acidophilic spherulocytes in the superficial and central dermis maintain their baseline levels up to the 2nd day, after which their numbers start to increase, reaching their highest values on the 4th day and returning to pre-injury levels by the 10th day. Thus, our results show that phagocytes and acidophilic spherulocytes presented fluctuations consistent with their physiological functions (i.e., tissue homeostasis) during the wound healing in *H. grisea.*

A few studies have identified phagocytes and acidophilic spherulocytes in the body wall of Holothuroidea (Eisapour et al., 2021; García-Arrarás et al., 2006; Miguel-Ruiz et al., 2007), but a large number of phagocytes were observed inside a blastema-like structure during intestinal regeneration in *H. parva* (Eisapour et al., 2021, described as "amebocytes"). The same cells may have been detected in the dermis of *H. glaberrima*, as the authors describe the presence of round bodies full of tattoo ink in the coelomic fluid and ink within the tissue, which was still observed after 28 days (Miguel-Ruiz et al., 2007). Since macrophages are responsible for maintaining tattoo ink in human skin (Baranska et al., 2018), the observation in *H. glaberrima* may result from phagocyte activity. Additionally, it was observed that connective phagocytes are responsible for collagen degradation in the compass depressor ligament of the sea urchin *P. lividus* (Sugni et al., 2014). For acidophilic spherulocytes, only two studies detected cells with similar characteristics in holothurian tissues (García-Arrarás et al., 2006; Miguel-Ruiz et al., 2007). The putative acidophilic spherulocytes observed in *H. glaberrima* show a grayish-blue colour in toluidine blue (Miguel-Ruiz et al., 2007, named as "spherulocytes"), which is quite similar to what is observed in *H. grisea* in the same stain (Queiroz et al., 2022a – Fig. 2E). It was noted that spherulocytes increase their number and show an unstructured morphology near the injured area during the wound healing process and the intestinal regeneration in *H. glaberrima* (García-Arrarás et al., 2006; Miguel-Ruiz et al., 2007). It was also observed that, in addition to the altered morphology, the fluorescent probe used to mark these cells can be found scattered in the injured region (Miguel-Ruiz et al., 2007), indicating the release of their contents. This aligns with our general findings and the function of these cells, which degranulate to release cytotoxic molecules (Vazzana et al., 2018).

During the wound healing process in *H. grisea*, the changes in phagocyte numbers suggest that these cells are recruited to the injury site to phagocytize debris and foreign particles. This explains the initial decrease in phagocytes in the superficial dermis, their continued increase in the hypodermis and their maintenance in the central dermis up to the 2ndday. Similarly, the changes in acidophilic spherulocyte numbers indicate their involvement in tissue defense due to their cytotoxic activity, but the onset of their activity is delayed compared to that of phagocytes. The continued decrease in hypodermic phagocytes during the first 24 h suggests an initial migration of local populations, followed by the recruitment of additional acidophilic spherulocytes. This explains their increase in all layers on the 2nd day and the sharp increase in the central and superficial dermis (i.e., the layers in which the injury is more severe) on the 4th day. This pattern aligns with the one observed in *H. glaberrima*, in which cell numbers decreased far from the injury and increased close to it (Miguel-Ruiz et al., 2007). From an integrated perspective, it seems plausible to assume that phagocytes and acidophilic spherulocytes act to maintain tissue integrity, supporting other processes such as tissue healing and remodeling.

Most studies on tissue healing have only recorded morula cells (Cowden, 1968; Menton and Eisen, 1970, 1973; Byrne, 1986; Lunetta and Michelucci, 2001; Miguel-Ruiz et al., 2007), while the contribution of fibroblast-like cells to wound healing has been poorly documented (Cowden, 1968; Menton and Eisen, 1973). It is also essential to highlight the potential involvement of phagocytes in tissue remodeling by degrading collagen fibers, as observed in *P. lividus* (Sugni et al., 2014). In *H. grisea,* fibroblast-like cells and morula cells promptly respond to tissue injury, although they show different patterns. Fibroblast-like cells in the superficial dermis sharply decrease in number during the first 12 h, returning to pre-injury levels on the 2nd day. Simultaneously, fibroblast-like cells in the central dermis and hypodermis remain near pre-injury levels with slight fluctuations during the first two days, show noteworthy alterations only on the 4th day, and then start to return to pre-injury levels on the 10th day. Morula cells show similar tendencies, but in an inverted pattern. Hypodermic morula cells sharply increase during the first 12 h and then decrease, reaching their lowest value on the 4th day and return to pre-injury levels from the 10th day on. In contrast, morula cells in the central and superficial dermis remain near pre-injury levels with slight fluctuations up to the 10th day, decrease to numbers close to zero on the 15th day and return to pre-injury levels only on the 30th day. As seen with phagocytes and acidophilic spherulocytes, the fluctuations observed in fibroblast-like cells and morula cells are consistent with their physiological functions (i.e., tissue healing and remodeling) during wound healing in *H. grisea.*

In *Sclerodactyla briareus* and *Isostichopus badionotus*, fibroblast-like cells are important during tissue healing (Cowden, 1968; Menton and Eisen, 1970, 1973), sometimes being the only cell type observed in the area (Cowden, 1968). In *I. badionotus,* it was noted that fibroblasts and new connective tissue fibers accumulated in a vertical arrangement in the injured region by the 2nd day, becoming more organized by the 4th day (Cowden, 1968). In *T. briareus*, fibroblasts were abundant in the non-injured superficial dermis, among the collagen laminae and in the injured area alongside morula cells (Menton and Eisen, 1973). In the sea urchin *P. lividus*, fibroblasts tested positive for prolyl 4-hydroxylase, which is a key enzyme in collagen synthesis (Sugni et al., 2014), indicating their participation in that process. Except for Cowden (1968), all studies on the connective morula cells of sea cucumbers have observed their presence and involvement in tissue healing/remodeling (Rollefsen, 1965; Menton and Eisen, 1970, 1973; Byrne, 1986; Miguel-Ruiz et al., 2007). In *Parastichopus tremulus*, *S. briareus* and *H. glaberrima*, morula cells were observed to increase in the injured area during wound healing (Rollefsen, 1965; Menton and Eisen, 1973; Miguel-Ruiz et al., 2007). A study on the fine structure of connective morula cells in *E. quiquesemita*

showed that: (1) the cytoplasmic spherules of morula cells are filled with glycosaminoglycans similar to those present in the connective tissue and (2) these cells can release their content into the extracellular matrix by degranulation, supporting the idea that they participate in the production of connective tissue and ground substances (Byrne, 1986). In *H. glaberrima*, the number of morula cells also increased in the injured area (Miguel-Ruiz et al., 2007), but their specific dynamics during wound healing differs from those observed here in *H. grisea*, probably due to the methods used to inflict the lesion. While part of the internal wall of the coelomic cavity was exposed and the incisions were made from the coelomic epithelia in the study on *H. glaberrima*, the injury was inflicted from the external surface in the present work.

Our results for fibroblast-like cells and morula cells in *H. grisea* align with previous studies (Menton and Eisen, 1973; Byrne, 1986; Miguel-Ruiz et al., 2007). Fibroblast-like cells in *H. grisea* are abundant in the superficial dermis and associated with new collagen fibers detected on the 2nd day and a denser connective tissue arrangement on the 4th day (cf., Fig. 7D and E). Meanwhile, morula cells increase in the injured area during the wound healing process. Thus, our data, along with data from previous studies, support the idea that both cell types are keystone participants in healing and remodeling the extracellular matrix (ECM). Morphofunctional and ultrastructural studies have also shown the involvement of morula cells in fibrogenesis (Menton and Eisen, 1973; Byrne, 1986; Miguel-Ruiz et al., 2007). However, interaction between fibroblast-like cells and morula cells is necessary to complete fibrogenesis and these might not be the only cell types responsible for this process. In vertebrates, fibroblasts play a central role during the wound healing process, being responsible for creating a new extracellular matrix that supports the other cells, among other functions (Bainbridge, 2013). In Holothuroidea, morula cells may be responsible for storing and releasing molecules that support the synthesis of new collagen fibers and the restoration of tissue structure by fibroblast-like cells.

4.3. *Understanding the interactions and dynamics of connective coelomocytes during the healing process*

At this point, the integration and complexity of the different processes occurring in the body wall of *H. grisea* during the wound healing

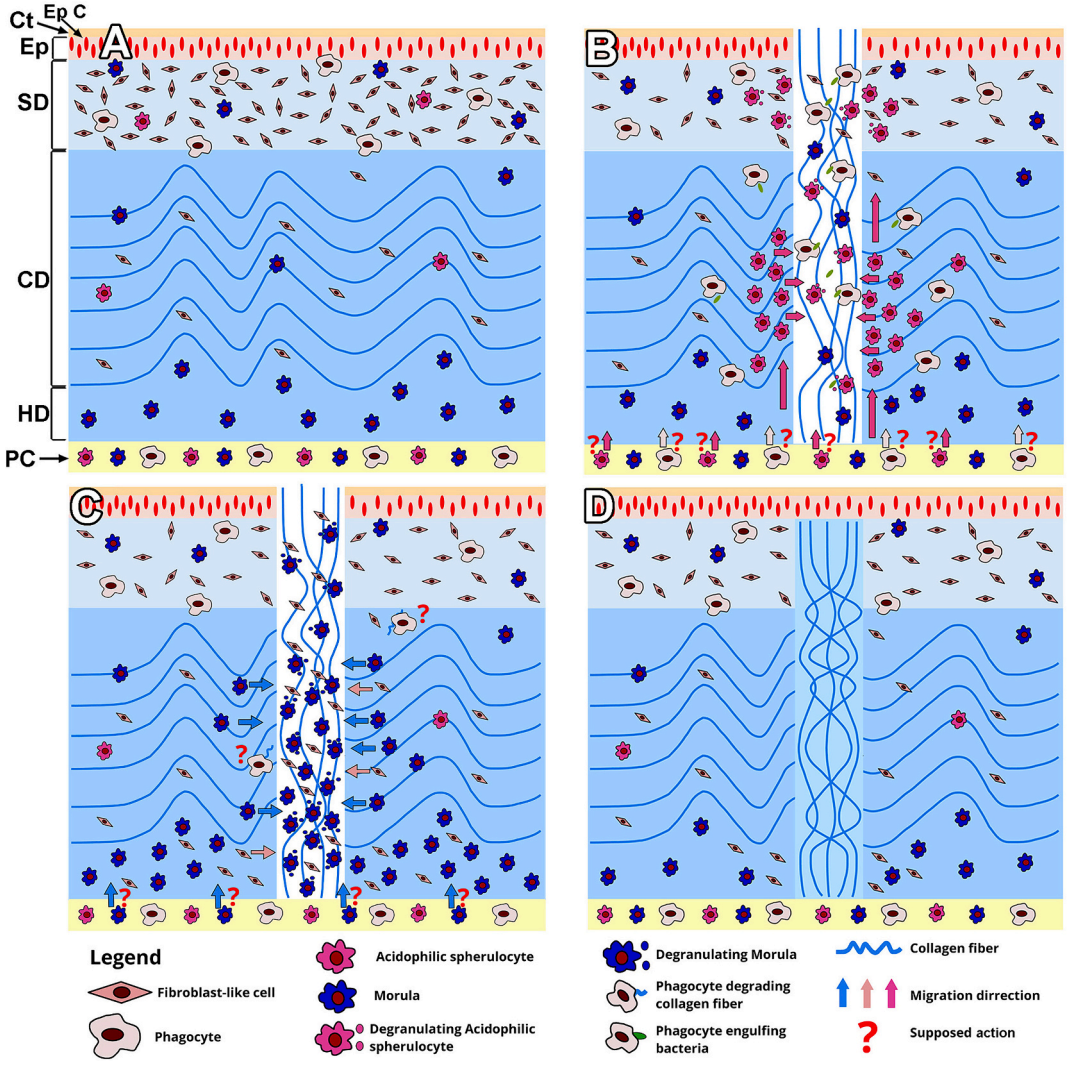

Fig. 9. Schematic representation of the main processes occurring during a wound-healing event in *Holothuria grisea*. A – Body wall before the injury, highlighting tissue organization and the main cell types; B – Homeostasis/clearance stage, highlighting the involvement of phagocytes and acidophilic spherulocytes in maintaining a sterile environment through the release of cytotoxic molecules and phagocytosis, respectively; C – Extracellular matrix (ECM) remodeling stage, highlighting the involvement of fibroblast-like cells, morula cells, and maybe phagocytes (?) in the reconstruction of the tissue; D – Healed tissue, highlighting the new ECM in a perpendicular position to the rest of the tissue. Note that although the processes highlighted in B and C had been explained separately in this scheme, they occur concomitantly. The colors of the cells are based on the colors they exhibit in Mallory trichrome preparations. Legend: Ct = Cuticle, Ep = Epidermis; Ep C = Epidermal cells; SD = Superficial dermis; CD = Central dermis; HD = Hypodermis; PC = Perivisceral coelom.

process are unquestionable. However, for a broader comprehension of this process, it is necessary to consider the main physiological responses occurring in the tissue (i.e., tissue homeostasis and ECM remodeling) as well as their timing and the dermal layers in which they occur. This process is summarized in Fig. 9. In uninjured animals, fibroblast-like cells and phagocytes are more numerous in the superficial dermis, while their numbers in the central dermis and hypodermis are considerably lower. In contrast, morula cells and acidophilic spherulocytes are more numerous in the hypodermis compared to the central and superficial dermis (Fig. 8 and 9A). After the injury, phagocytes and acidophilic spherulocytes become committed to tissue homeostasis/clearance, with the former removing debris and foreign particles and the latter releasing cytotoxic compounds into the tissue to counter potential invaders (Fig. 9B). However, while phagocytes are quickly recruited, the activity of acidophilic spherulocytes is delayed. This explains the decrease of phagocyte numbers in the superficial dermis concomitant with their increase in the central dermis and hypodermis during the first 12 h and their significant increase in the superficial and central dermis only on the 4th day (Fig. 9B).

The activity of phagocytes and acidophilic spherulocytes in maintaining a sterile *milieu intérieur* coincides with the activity of fibroblast-like cells, morula cells and possibly additional phagocytes in degrading old collagen fibers to reconstruct the ECM. Morula cells may be responsible for storing and releasing the molecules that will be used by fibroblast-like cells to create and organize new collagen fibers, thus restoring the tissue structure (Fig. 9C). By the 10th day, the wound is already closed and, although the ECM is not entirely structured, the tissue shows a highly organized arrangement, suggesting that the animal can return to its natural activity. At this stage, the number of connective coelomocytes returns to basal levels (Fig. 9D). To some extent, the events observed during wound healing in *H. grisea* resembles those observed in mammals (Muire et al., 2022). While the inflammatory and proliferative phases of wound healing are temporally separated in mammals (Muire et al., 2022), this does not appear to be the case in *H. grisea*. The inflammation-like phase of *H. grisea*, characterized by the migration of phagocytes and acidophilic spherulocytes, is evident 12 h post-injury. The migration of fibroblast-like cells and morula cells, the events that characterize the proliferation-like phase of *H. grisea*, can also be observed during this time. Finally, the remodeling phase can be observed on day 4, which appears to be faster than in mammals (Muire et al., 2022). It is important to emphasize that no granulation-like tissue was observed in *H. grisea*.

Although our study provides evidence of connective coelomocyte function and dynamics during the wound healing process, one crucial question remains unsolved: Where do the coelomocytes that appear in the connective tissue come from? More specifically, do these cells originate in the tissue itself or do they come from another location? Previous studies have failed to detect cell proliferation in the connective coelomocytes during the initial phase of the wound healing process (Cowden, 1968; Menton and Eisen, 1973; Miguel-Ruiz et al., 2007). In fact, the most complete study on this topic (Miguel-Ruiz et al., 2007) showed that cell proliferation in the coelomic epithelia of *H. glaberrima*, suggested to be a “coelomopoietic” site (Bossche and Jangoux, 1976; Guatelli et al., 2022), becomes significant only in the 6th day post-injury. However, as demonstrated here and in other studies (Cowden, 1968; Menton and Eisen, 1973; Miguel-Ruiz et al., 2007), most steps necessary for the healing and closure of the wound are already advanced by this time. Thus, we suspect that at least morula cells, but probably other cell types as well, may migrate from the coelom to the injured tissue to aid in the wound healing process, at least during its initial phase, similar to the leukocyte diapedesis observed in mammals (Petri and Bixel, 2006). The decrease in perivisceral morula cells within 6-12 h, followed by their increase in the hypodermis, supports this suggestion. However, we are aware that this hypothesis requires further studies to be confirmed.

5. Conclusions

Regeneration in Echinodermata has caught the attention of researchers since the early twentieth century and the tissue/gut recovery after evisceration is a relatively well-understood process in Holothuroidea (García-Arrarás and Greenberg, 2001; Mashanov and García-Arrarás, 2011; Su et al., 2022). However, tissue healing, a process distinct from total intestinal regrowth, has been poorly studied. Here, we observed that perivisceral responses to external damage are faster than tissue responses. Coelomic alterations could be detected as early as 1 h post-injury (viz., neutral red uptake), most of the changes became apparent 3 h post-injury and the return to pre-injury levels took only two days. We also highlight that the combination of cellular and humoral parameters successfully helped in monitoring the health of the sea cucumbers during the initial phase of wound healing.

Unlike perivisceral responses, tissue responses require more time to be initiated, as illustrated by the acidophilic spherulocyte dynamics, and even more time to be completed, reaching pre-injury levels only on the 10th day. We also observed that connective coelomocytes probably cooperate in different but complementary processes, with phagocytes and acidophilic spherulocytes being involved in tissue clearance and homeostasis, while morula cells and fibroblasts (and possibly phagocytes) participate in tissue healing and ECM remodeling. Our results also show that the main phases observed in mammalian wound healing may be seen in *H. grisea*. Lastly, our study demonstrates that an integrated approach was essential to provide a broader understanding of the physiological responses in both the perivisceral coelom and tissue during the wound healing process of *Holothuria grisea*, highlighting the alterations that occurred in both compartments and a potential interaction between them.

Supplementary data to this article can be found online at https://doi.org/10.1016/j.cbpa.2024.111695.

Funding

This study was supported by the Fundação de Amparo à Pesquisa do Estado de São Paulo - FAPESP (Grant numbers: 2008/07189-3, 2015/21460-5, 2018/14497-8, 2021/10161-8, and 2024/05857-1), Conselho Nacional de DesenvolvimentoCientífico e Tecnológico - CNPq (306960/2023-0), and Coordenação de Aperfeiçoamento de Pessoal de Nível Superior-CAPES.

CRediT authorship contribution statement

Patrícia Lacouth: Writing – original draft, Validation, Methodology, Investigation, Conceptualization. **Alessandra Majer:** Writing – review & editing, Methodology, Formal analysis. **Vincenzo Arizza:** Writing – review & editing, Methodology. **Mirella Vazzana:** Writing – review & editing, Methodology. **Manuela Mauro:** Writing – review & editing, Methodology. **Márcio Reis Custódio:** Writing – review & editing, Supervision, Resources, Methodology, Conceptualization. **Vinicius Queiroz:** Writing – review & editing, Writing – original draft, Validation, Methodology, Data curation, Conceptualization.

Declaration of competing interest

The authors declare that they have no known competing interests or personal relationships that could have appeared to influence the work reported in this study.

Data availability

Data will be made available on request.

Acknowledgments

The authors thank the staff of the Centro de Biologia Marinha (CEBIMar-USP) for the provision of laboratory facilities and technical support during field trips; and the Fundação de Amparo à Pesquisa do Estado de São Paulo - FAPESP, Conselho Nacional de Desenvolvimento Científico e Tecnológico - CNPq, and the Coordenação de Aperfeiçoamento de Pessoal de Nível Superior-CAPES for financial support. This is a contribution of the NP-BioMar (Research Center for Marine Biodiversity - USP).

References

Agata, K., Saito, Y., Nakajima, E., 2007. Unifying principles of regeneration I: epimorphosis versus morphallaxis. Develop. Growth Differ. 49 (2), 73–78.
Arizza, V., Giaramita, F.T., Parrinello, D., Cammarata, M., Parrinello, N., 2007. Cell cooperation in coelomocyte cytotoxic activity of *Paracentrotus lividus* coelomocytes. Comp. Biochem. Phys. A – Mol. Integ. Phys. 147 (2), 389–394.
Arizza, V., Vazzana, M., Schillaci, D., Russo, D., Giaramita, F.T., Parrinello, N., 2013. Gender differences in the immune system activities of sea urchin *Paracentrotus lividus*. Comp. Biochem. Phys. A – Mol. Integ. Phys. 164 (3), 447–455.
Ates, G., Vanhaecke, T., Rogiers, V., Rodrigues, R.M., 2017. Assaying cellular viability using the neutral red uptake assay. Methods Mol. Biol. 1601, 19–26.
Bainbridge, P., 2013. Wound healing and the role of fibroblasts. J. Wound Care 22 (8), 407–412.
Baranska, A., Shawket, A., Jouve, M., Baratin, M., Malosse, C., Voluzan, O., Malissen, B., 2018. Unveiling skin macrophage dynamics explains both tattoo persistence and strenuous removal. J. Exp. Med. 215 (4), 1115–1133.
Behmer, O.A., Tolosa, E.M.C., Freitas-Neto, A.G., 1976. Manual de técnicas de histologia normal e patológica. EDART/EDUSP, São Paulo.
Bergmeier, W., Wagner, D.D., 2007. 2007. Inflammation. In: Michelson, A.D. (Ed.), Platelets (2nd Ed.). Elsevier, Boston, MA, pp. 713–726.
Bossche, J.P.V., Jangoux, M., 1976. Epithelial origin of starfish coelomocytes. Nature 261 (5557), 227–228.
Bradford, M.M., 1976. A rapid and sensitive method for the quantitation of microgram quantities of protein utilizing the principle of protein-dye binding. Anal. Biochem. 72, 248–254.
Byrne, M., 1986. The ultrastructure of the morula cells of *Eupentacta quinquesemita* (Echinodermata: Holothuroidea) and their role in the maintenance of the extracellular matrix. J. Morphol. 188 (2), 179–189.
Canicattì, C., 1988. The lytic system of *Holothuria polii* (Echinodermata): a review. Ital. J. Zool. 55 (1–4), 139–144.
Canicattì, C., Parrinello, N., 1985. Hemagglutinin and hemolysin levels in the coelomic fluid from *Holothuria polii* (Echinodermata) following sheep erythrocyte injection. Biol. Bull. 168 (1), 175–182.
Chiaramonte, M., Inguglia, L., Vazzana, M., Deidun, A., Arizza, V., 2019. Stress and immune response to bacterial LPS in the sea urchin *Paracentrotus lividus* (Lamarck, 1816). Fish Shellfish Immunol. 92, 384–394.
Chou, H.Y., Lun, C.M., Smith, L.C., 2018. SpTransformer proteins from the purple sea urchin opsonize bacteria, augment phagocytosis, and retard bacterial growth. PLoS One 13 (5), e0196890.
Cigliola, V., Ghila, L., Chera, S., Herrera, P.L., 2020. Tissue repair brakes: a common paradigm in the biology of regeneration. Stem Cells 38 (3), 330–339.
Clow, L.A., Raftos, D.A., Gross, P.S., Smith, L.C., 2004. The sea urchin complement homologue, SpC3, functions as an opsonin. J. Exp. Biol. 207 (12), 2147–2155.
Cowden, R.R., 1968. Cytological and histochemical observations on connective tissue cells and cutaneous wound healing in the sea cucumber *Stichopus badionotus*. J. Invertebr. Pathol. 10 (1), 151–159.
Daponte, V., Tylzanowski, P., Forlino, A., 2021. Appendage regeneration in vertebrates: what makes this possible? Cells 10 (2), 242.
Ding, K., Zhang, L., Huo, D., Guo, X., Liu, X., Zhang, S., 2021. Metabolomic analysis of coelomic fluids reveals the physiological mechanisms underlying evisceration behavior in the sea cucumber *Apostichopus japonicus*. Aquaculture 543, 736960.
Dolmatov, I.Y., 2021. Molecular aspects of regeneration mechanisms in holothurians. Genes 12 (2), 250.
Dunham, P., Weissmann, G., 1986. Aggregation of marine sponge cells induced by ca pulses, ca ionophores, and phorbol esters proceeds in the absence of external ca. Biochem. Bioph. Res. Co. 134 (3), 1319–1326.
Dupont, S., Thorndyke, M., 2007. Bridging the regeneration gap: insights from echinoderm models. Nat. Rev. Genet. 8 (4), 320.
Dvorak, H.F., 2015. Tumors: wounds that do not heal–redux. Cancer Immunol. Res. 3, 1–11.
Eisapour, M., Salamat, N., Salari, M.A., Bahabadi, M.N., Salati, A.P., 2021. Digestive tract regeneration in the posteriorly eviscerating sea cucumber *Holothuria parva* (Holothuroidea, Echinodermata). Zoomorphology 140 (1), 69–83.
Eliseikina, M.A., Magarlamov, T.Y., 2002. Coelomocyte morphology in the holothurians *Apostichopus japonicus* (Aspidochirota: Stichopodidae) and *Cucumaria japonica* (Dendrochirota: Cucumariidae). Russ. J. Mar. Biol. 28 (3), 197–202.
Ellington, W.R., Lawrence, J.M., 1974. Coelomic fluid volume regulation and isosmotic intracellular regulation by *Luidia clathrata* (Echinodermata: Asteroidea) in response to hyposmotic stress. Biol. Bull. 146 (1), 20–31.
Ereskovsky, A., Borisenko, I.E., Bolshakov, F.V., Lavrov, A.I., 2021. Whole-body regeneration in sponges: diversity, fine mechanisms, and future prospects. Genes 12 (4), 506.
Figueiredo, D.A.L., Branco, P.C., Dos Santos, D.A., Emerenciano, A.K., Iunes, R.S., Borges, J.C.S., da Silva, J.R.M.C., 2016. Ocean acidification affects parameters of immune response and extracellular pH in tropical sea urchins *Lytechinus variegatus* and *Echinometra lucunter*. Aquat. Toxicol. 180, 84–94.
Freshney, R., 1987. Culture of Animal Cells: A Manual of Basic Technique. Alan R. Liss (org), Inc, New York.
García-Arrarás, J.E., Greenberg, M.J., 2001. Visceral regeneration in holothurians. Microsc. Res. Tech. 55 (6), 438–451.
García-Arrarás, J.E., Schenk, C., Rodrígues-Ramírez, R., Torres, I.I., Valentín, G., Candelaria, A.G., 2006. Spherulocytes in the echinoderm *Holothuria glaberrima* and their involvement in intestinal regeneration. Dev. Dyn. 235 (12), 3259–3267.
Guatelli, S., Ferrario, C., Bonasoro, F., Anjo, S.I., Manadas, B., Candia Carnevali, M.D., Sugni, M., 2022. More than a simple epithelial layer: multifunctional role of echinoderm coelomic epithelium. Cell Tissue Res. 390 (2), 207–227.
Guerrero, A.G., Forero, A.R., 2018. Histological characterization of skin and radial bodies of two species of genus *Isostichopus* (Echinodermata: Holothuroidea). Egypt. J. Aquat. Res. 44 (2), 155–161.
Hamel, J.F., Jobson, S., Caulier, G., Mercier, A., 2021. Evidence of anticipatory immune and hormonal responses to predation risk in an echinoderm. Sci. Rep. 11 (1), 1–10.
Jellett, J.F., Wardlaw, A.C., Scheibling, R.E., 1988. Experimental infection of the echinoid *Strongylocentrotus droebachiensis* with *Paramoeba invadens*: quantitative changes in the coelomic fluid. Dis. Aquat. Org. 4, 149–157.
Johnstone, C.R., 2015. Investigation of Coelomic Fluid from the Sea Urchin *E. chloroticus* (Doctoral dissertation, University of Otago), p. 168.
Kale, R.D., Krishnamoorthy, R.V., 1979. Comparative account of coelomocytes and haemocytes of five species of earthworms. Proc. Indian Acad. Sci. 88, 329–337.
Kun, X., Yang, H., 2009. Phagocytosis by amoebocytes in *Apostichopus japonicus*. SPC Beche-de-mer Information Bulletin 29, 44–46.
Li, Q., Ren, Y., Liang, C., Qiao, G., Wang, Y., Ye, S., Li, R., 2018. Regeneration of coelomocytes after evisceration in the sea cucumber, *Apostichopus japonicus*. Fish Shellfish Immunol. 76, 266–271.
Lunetta, G.D.A., Michelucci, M.L., 2001. Engagement of the periesophageal ring during *Holothuria polii* response to erythrocyte injection. Eur. J. Histochem. 46 (2), 185–194.
Mahar, M., Cavalli, V., 2018. Intrinsic mechanisms of neuronal axon regeneration. Nat. Rev. Neurosci. 19 (6), 323–337.
Mashanov, V.S., García-Arrarás, J.E., 2011. Gut regeneration in holothurians: a snapshot of recent developments. Biol. Bull. 221 (1), 93–109.
Mauro, M., Queiroz, V., Arizza, V., Campobello, D., Custódio, M.R., Chiaramonte, M., Vazzana, M., 2021. Humoral responses during wound healing in *Holothuria tubulosa* (Gmelin, 1788). Comp. Biochem. Physiol. B Biochem. Mol. Biol. 253, 110550.
McClay, D.R., 2011. Evolutionary crossroads in developmental biology: sea urchins. Develop 138 (13), 2639–2648.
McMillan, D.B., Harris, R.J., 2018. An Atlas of Comparative Vertebrate Histology, pp. 75–117. https://doi.org/10.1016/b978-0-12-410424-2.00004-4.
Melo, R.F., Martin, S.S., Sommerhoff, C.P., Pejler, G., 2019. Exosome-mediated uptake of mast cell tryptase into the nucleus of melanoma cells: a novel axis for regulating tumor cell proliferation and gene expression. Cell Death Dis. 10 (9), 659.
Menton, D.N., Eisen, A.Z., 1970. The structure of the integument of the sea cucumber, *Thyone briareus*. J. Morphol. 131 (1), 17–35.
Menton, D.N., Eisen, A.Z., 1973. Cutaneous wound healing in the sea cucumber, *Thyone briareus*. J. Morphol. 141 (2), 185–203.
Miguel-Ruiz, S., José, E., García-Arrarás, J.E., 2007. Common cellular events occur during wound healing and organ regeneration in the sea cucumber *Holothuria glaberrima*. BMC Dev. Biol. 7 (1), 1–19.
Muire, P.J., Thompson, M.A., Christy, R.J., Natesan, S., 2022. Advances in immunomodulation and immune engineering approaches to improve healing of extremity wounds. Int. J. Mol. Sci. 23 (8), 4074.
Murano, C., Bergami, E., Liberatori, G., Palumbo, A., Corsi, I., 2021. Interplay between nanoplastics and the immune system of the mediterranean sea urchin *Paracentrotus lividus*. Front. Mar. Sci. 8, 647394.
Pearse, J.S., 1967. Coelomic water volume control in the Antarctic Sea-star *Odontaster validus*. Nature 216 (5120), 1118–1119.
Peterson, K.J., Eernisse, D.J., 2016. The phylogeny, evolutionary developmental biology, and paleobiology of the Deuterostomia: 25 years of new techniques, new discoveries, and new ideas. Org. Divers. Evol. 16, 401–418.
Petri, B., Bixel, M.G., 2006. Molecular events during leukocyte diapedesis. FEBS J. 273 (19), 4399–4407.
Pinsino, A., Alijagic, A., 2019. Sea urchin *Paracentrotus lividus* immune cells in culture: formulation of the appropriate harvesting and culture media and maintenance conditions. Biol. Open. 8 (3), bio039289.
Prompoon, Y., Weerachatyanukul, W., Withyachumnarnkul, B., Vanichviriyakit, R., Wongprasert, K., Asuvapongpatana, S., 2015. Lectin-based profiling of coelomocytes in *Holothuria scabra* and expression of superoxide dismutase in purified coelomocytes. Zool. Sci. 32 (4), 345–351.
Queiroz, V., 2020. An unprecedented association of an encrusting bryozoan on the test of a live sea urchin: epibiotic relationship and physiological responses. Mar. Biodivers. 50 (5), 1–7.
Queiroz, V., Custódio, M.R., 2024. Diversity of coelomocytes in the class Holothuroidea, 377–401 pp. In: Mercier, A., Hamel, J.-F., Suhrbier, A., Pearce, C. (Eds.), The World of Sea Cucumbers. Academic Press.

Queiroz, V., Mauro, M., Arizza, V., Custódio, M.R., Vazzana, M., 2022a. The use of an integrative approach to identify coelomocytes in three species of the genus *Holothuria* (Echinodermata). Invertebr. Biol. 141 (1), e12357.
Queiroz, V., Arizza, V., Vazzana, M., Custódio, M.R., 2022b. Comparative evaluation of coelomocytes in *Paracentrotus* Sea urchins: description of new cell types and insights on spherulocyte maturation and sea urchin physiology. Zool. Anz. 300, 27–40.
Ramírez-Gómez, F., Aponte-Rivera, F., Méndez-Castaner, L., García-Arrarás, J.E., 2010. Changes in holothurian coelomocyte populations following immune stimulation with different molecular patterns. Fish Shellfish Immunol. 29 (2), 175–185.
Reddien, P.W., 2018. The cellular and molecular basis for planarian regeneration. Cell 175 (2), 327–345.
Reule, S., Gupta, S., 2011. Kidney regeneration and resident stem cells. Organogenesis 7 (2), 135–139.
Rollefsen, I., 1965. Studies on the mast cell-like morula cells of the Holothurian *Stichopus hemulus* (qun.). In: Arb. Univ. Bergen. Mat. Naturv. Serie no. 8, Oslo, pp. 1–19.
Saló, E., Baguñà, J., 2002. Regeneration in planarians and other worms: new findings, new tools, and new perspectives. J. Exp. Zool. 292 (6), 528–539.
Shannon, R., Mustafa, A., 2015. A comparison of stress susceptibility of sea urchins and sea cucumbers in aquaculture conditions. Bioeng. Biosci 3, 100–107.
Silva, J.R.M.C., 2013. Immunology in sea urchins. In: Lawrence, J.M. (Ed.), Sea Urchins: Biology and Ecology, 3rd edition. Academic Press, United Kingdom, pp. 187–194.
Silva, J.E.B., Boleli, I.C., Simões, Z.L.P., 2002. Hemocyte types and total and differential counts in unparasitized and parasitized *Anastrepha obliqua* (Diptera, Tephritidae) larvae. Braz. J. Biol. 62, 689–699.
Stabili, L., Acquaviva, M.I., Cavallo, R.A., Gerardi, C., Narracci, M., Pagliara, P., 2018. Screening of three echinoderm species as new opportunity for drug discovery: their bioactivities and antimicrobial properties. J. Evid. Based Complement. Altern. Med. 1–8.
Strober, W., 2015. Trypan blue exclusion test of cell viability. Curr. Protoc. Immunol. 111. A3.B.1–A3.B.3.
Su, F., Yang, H., Sun, L., 2022. A review of histocytological events and molecular mechanisms involved in intestine regeneration in holothurians. Biol 11, 1095.
Sugni, M., Fassini, D., Barbaglio, A., Biressi, A., Di Benedetto, C., Tricarico, S., Carnevali, M.D.C., 2014. Comparing dynamic connective tissue in echinoderms and sponges: morphological and mechanical aspects and environmental sensitivity. Mar. Environ. Res. 93, 123–132.
Taguchi, M., Tsutsui, S., Nakamura, O., 2016. Differential count and time-course analysis of the cellular composition of coelomocyte aggregate of the Japanese sea cucumber *Apostichopus japonicus*. Fish Shellfish Immunol. 58, 203–209.
Thorndyke, M.C., Chen, W.C., Moss, C., Carnevali, M.D.C., Bonasoro, F., 2001. Regeneration in echinoderms: Cellular and molecular aspects. In: Carnevali, D., Bonoasoro, F. (Eds.), Echinoderm Research. Balkema, Rotterdam, pp. 159–164.
Ura, K., Takei, N., Higuchi, I., Yuhi, T., Nishimiya, O., Takagi, Y., 2017. Changes in levels of major yolk protein in the coelomic fluid and gonad during the reproductive cycle in wild sea urchins, Mesocentrotus nudus. BioRxiv 241059.
Vázquez-Vélez, G.E., Rodríguez-Molina, J.F., Quiñones-Frías, M.C., Pagán, M., García-Arrarás, J.E., 2016. A proteoglycan-like molecule offers insights into ground substance changes during holothurian intestinal regeneration. J. Histochem. Cytochem. 64 (6), 381–393.
Vazzana, M., Siragusa, T., Arizza, V., Buscaino, G., Celi, M., 2015. Cellular responses and HSP70 expression during wound healing in *Holothuria tubulosa* (Gmelin, 1788). Fish Shellfish Immunol. 42 (2), 306–315.
Vazzana, M., Celi, M., Chiaramonte, M., Inguglia, L., Russo, D., Ferrantelli, V., Battaglia, D., Arizza, V., 2018. Cytotoxic activity of *Holothuria tubulosa* (Echinodermata) coelomocytes. Fish & shellfish immunol 72, 334–341.
Vazzana, M., Mauro, M., Ceraulo, M., Dioguardi, M., Papale, E., Mazzola, S., Buscaino, G., 2020. Underwater high frequency noise: biological responses in sea urchin *Arbacia lixula* (Linnaeus, 1758). Comp. Biochem. Physiol. - Part A: Mol. Integ. Phys. 242, 110650.
Wahltinez, S.J., Newton, A.L., Harms, C.A., Lahner, L.L., Stacy, N.I., 2020. Coelomic fluid evaluation in *Pisaster ochraceus* affected by sea star wasting syndrome: evidence of osmodysregulation, calcium homeostasis derangement, and coelomocyte responses. Fron.Vet. Sci. 7, 131.
Wong, A.Y., Whited, J.L., 2020. Parallels between wound healing, epimorphic regeneration and solid tumors. Development 147 (1), dev181636.
Xing, K., Yang, H.S., Chen, M.Y., 2008. Morphological and ultrastructural characterization of the coelomocytes in *Apostichopus japonicus*. Aquat. Biol. 2 (1), 85–92.
Yui, M.A., Bayne, C.J., 1983. Echinoderm immunology: bacterial clearance by the sea urchin *Strongylocentrotus purpuratus*. Biol. Bull. 165 (2), 473–486.
Zang, Y., Tian, X., Dong, S., Dong, Y., 2012. Growth, metabolism and immune responses to evisceration and the regeneration of viscera in sea cucumber, *Apostichopus japonicus*. Aquaculture 358, 50–60.
Zhang, X., Sun, L., Yuan, J., Sun, Y., Gao, Y., Zhang, L., Xiang, J., 2017. The sea cucumber genome provides insights into morphological evolution and visceral regeneration. PLoS Biol. 15 (10), e2003790.